NMR studies on heavy fermion and conventional metal superlattices $CeCoIn_5/YbCoIn_5$

2017 J. Phys.: Conf. Ser. 807 012004

(http://iopscience.iop.org/1742-6596/807/1/012004)

NMR studies on heavy fermion and conventional metal superlattices $CeCoIn_5/YbCoIn_5$

T. Yamanaka[1], M. Shimozawa[2], R. Endo[1], Y. Mizukami[3], H. Shishido[4]. T. Terashima[5], T. Shibauchi[1,3], Y. Matsuda[1], K. Ishida[1]

[1]Department of Physics, Kyoto University, Kyoto 606-8502, Japan
[2]Institute for Solid State Physics, University of Tokyo, Kashiwa, Chiba 277-8581, Japan
[3]Department of Advanced Materials Science, University of Tokyo, Kashiwa, Chiba 277-8561, Japan
[4]Department of Physics and Electronics, Osaka Prefecture University, Sakai, Osaka 599-8531, Japan
[5]Research Center for Low Temperature and Materials Sciences, Kyoto University, Kyoto 606-8501, Japan

E-mail: `t-yamanaka@scphys.kyoto-u.ac.jp`

Abstract.
We performed nuclear magnetic resonance (NMR) experiments on heavy fermion and conventional metal superlattices $CeCoIn_5/YbCoIn_5$. We succeeded in identifying the signals arising from $CeCoIn_5$ and $YbCoIn_5$ block layers (BLs) by comparing the spectra of the $CeCoIn_5/YbCoIn_5$ superlattices, $CeCoIn_5$ thin film, and $YbCoIn_5$ thin film. Furthermore, we found that the signals of Ce-BLs could be divided into signals arising from interfacial layers and inner layers even in one Ce-BL by comparing the spectra of two $CeCoIn_5/YbCoIn_5$ superlattices with different thickness of the Ce-BLs. A comparison of the spectra of the superlattices with different Ce-BL thickness and field dependence of nuclear-spin lattice relaxation rate $1/T_1$ indicate that antiferromagnetic spin fluctuations at the interfacial site are more suppressed than those at the inner layer site even in the Ce-BLs.

1. Introduction

The physics of strongly correlated electron systems is remarkably rich, and in such materials the entanglement of charge, spin, and orbital degrees of freedom often causes the emergence of exotic quantum phases. It has been shown that in the presence of exotic spin-orbit interaction, spatial inversion symmetry breaking can produce notable effects on these systems through a Fermi surface splitting with different spin structures even in the absence of a magnetic field, giving rise to a plethora of novel phenomena such as anomalous magnetoelectric effects[1, 2] and topological superconducting states[3, 4, 5]. In addition, it has been shown that the electronic properties are changed at the interface of different compounds at which the inversion symmetry is locally broken, even when the global inversion symmetry is preserved in the whole crystal[6]. Among others, the metallic state with the strongest electron correlation is realized in the heavy-fermion systems. Recently, the technique of fabricating epitaxial superlattices consisting of heavy-fermion compounds and conventional metals has been developed and provides us a unique research field to study the interplay between locally inversion symmetry breaking and the heavy-fermion characters[7, 8, 9].

$CeCoIn_5$ [Fig.1(a)], one of the constituents of the $CeCoIn_5/YbCoIn_5$ superlattices studied here, has the highest superconducting transition temperature $T_c = 2.3$ K [10] among Ce-based heavy-fermion superconductors and the superconducting gap symmetry of $CeCoIn_5$ is considered as $d_{x^2-y^2}$[11, 12, 13, 14]. The Cd- and Hg-substituted $CeCoIn_5$ show antiferromagnetic (AFM) ordering[15, 16] and therefore $CeCoIn_5$ is also considered to be located at the vicinity of AFM quantum critical point. These facts suggest that the superconductivity in $CeCoIn_5$ is mediated by AFM fluctuations. $YbCoIn_5$, the other constituent of the $CeCoIn_5/YbCoIn_5$ superlattices, exhibits Fermi liquid behavior in electrical resistivity and magnetic susceptibility[17], indicating that the Yb ions in $YbCoIn_5$ are divalent ions with the closed-shell $4f^{14}$ configuration[18].

In $CeCoIn_5/YbCoIn_5$ superlattices, highly unusual superconducting properties such as the enhanced anisotropy of the upper critical field H_{c2}[8] and anomalous enhancement of H_{c2} regardless of T_c decrease have been observed[19, 20], in particular when the thickness of the Ce-block layers (BLs) is only a few unit cells. Although the importance of the interfaces between Ce- and Yb-BLs has been reported, it is difficult to investigate their physical properties at the microscopic level. Recently, we reported nuclear magnetic resonance (NMR) studies on the $CeCoIn_5/YbCoIn_5$ superlattices, in which we found that the $1/T_1T$ of Ce-BLs was suppressed with decreasing Ce-BL thickness, whereas that of Yb-BLs essentially the same as $YbCoIn_5$ thin film[21]. In this paper, we discuss the NMR-spectrum difference in different Ce-BL thickness and show that the NMR spectra of Ce-BLs in $CeCoIn_5/YbCoIn_5$ superlattices can be divided into the signals arising from interfacial and inner layers.

2. Experimental

We have performed NMR measurements on two thin films of $CeCoIn_5$ and $YbCoIn_5$, and two superlattices $CeCoIn_5(n)/YbCoIn_5(5)$, where $n(= 5$ and $9)$ layers of $CeCoIn_5$ and 5 layers of $YbCoIn_5$ were stacked alternately[Fig. 1(b)]. In the NMR measurements, the frequency was fixed at 114.5 MHz and the magnetic field was applied along the c axis. The samples were grown by molecular beam epitaxial technique[8], and the set of $CeCoIn_5(n)$ and $YbCoIn_5(5)$ in the $CeCoIn_5(n)/YbCoIn_5(5)$ samples repeats 40 times for $n = 5$ and 30 times for $n = 9$. The thickness of the thin films of $CeCoIn_5$ and $YbCoIn_5$ are 500 nm ($\approx$ 600 unit cell layers) and 350 nm ($\approx$ 400 unit cell layers), respectively. The $CeCoIn_5$ thin film was grown on MgF_2 substrate directly. The $YbCoIn_5$ thin film has $CeIn_3$ buffer layers on MgF_2 substrate, and the $CeCoIn_5(n)/YbCoIn_5(5)$ superlattices have $CeIn_3$(28 nm) and $YbCoIn_5$(15-unit-cell thick) as buffer layers.

3. Results and discussions

NMR is one of the most suitable microscopic probes, providing BL-selective information on the magnetic properties. Panels of FIG. 1(c) depict the NMR spectra of the $n = 9$ and $n = 5$ superlattices for $\boldsymbol{H} \parallel c$, together with the spectra of $CeCoIn_5$ [top] and $YbCoIn_5$ [bottom] thin films. From detailed analysis of the field swept spectra we are able to obtain the site-selective NMR information, i.e. spectroscopic information resolved for the Ce- and Yb-BLs separately. In the thin films of $CeCoIn_5$ and $YbCoIn_5$, NMR signals arising from two In sites, In(1) located at the center of the Ce/Yb-In layer and In(2) site located on the lateral faces, and Co site can be clearly identified and be reproduced by NMR-line simulation with the parameters shown in Table I. The parameters of bulk $CeCoIn_5$ are approximately the same values reported in some papers[22, 23, 24]. The largest principal axis of the electric field gradient is parallel to the c axis at the In(1) and Co sites, while it is perpendicular to the lateral face at the In(2) site.

Here we focus on the spectra arising from the central transition ($+1/2 \leftrightarrow -1/2$) of the In(1) site, as shown in panels of FIG. 1(d), which are expanded views in the field range between 11.9 T and 12.4 T. It should be noted that the spectra of the $n = 9$ and $n = 5$ superlattices consist of the spectra of the Ce- and Yb-BLs. Indeed, the positions of the spectra pointed by red and

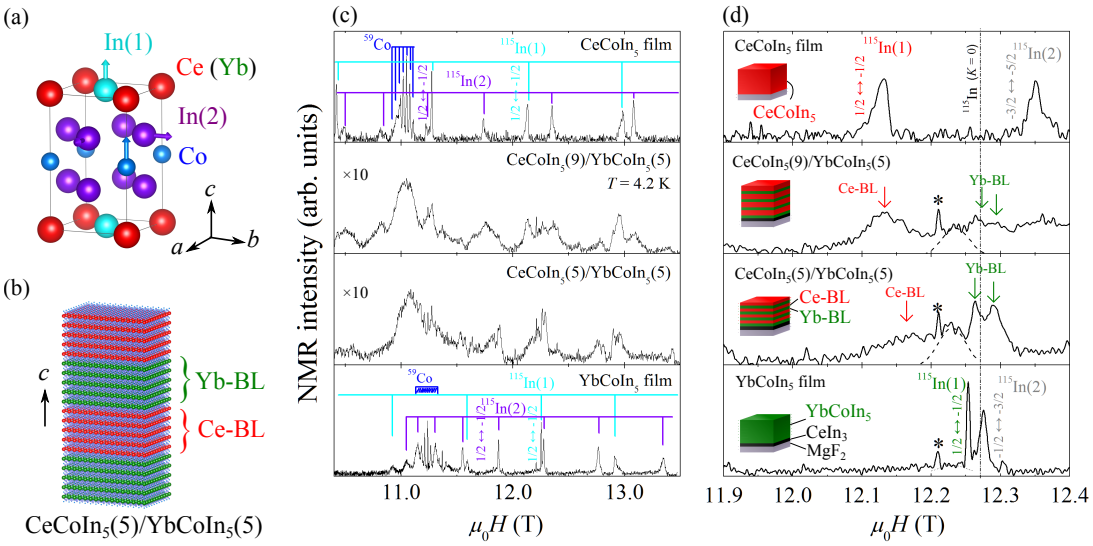

Figure 1. (a) Crystal structure of $R(=$ Ce, Yb)$CoIn_5$.(b) Schematic image of the $CeCoIn_5(5)/YbCoIn_5(5)$ superlattice. (c) Field swept NMR spectra of $CeCoIn_5$ thin film, $CeCoIn_5(9)/YbCoIn_5(5)$ superlattice, $CeCoIn_5(5)/YbCoIn_5(5)$ superlattice, and $YbCoIn_5$ thin films at 4.2 K. (d) Expanded views of NMR spectra from $\mu_0 H = 11.9$ T to 12.4 T of each sample. The signals around 12.22 T pointed by asterisks and dashed lines arise from the buffer layers of $CeIn_3$.

Table 1. NMR parameters of the $CeCoIn_5$ and $YbCoIn_5$ thin films, i.e. Knight shift along the c axis(K_c), electric quadrupole frequency(ν_Q), and asymmetric parameter of the electric quadrupole interaction (η) at Co, In(1), and In(2) sites.

Nucleus	Sample	K_c (%)	ν_Q (MHz)	η
^{59}Co	$CeCoIn_5$ bulk	3.39	0.230	0
	$CeCoIn_5$ film	3.58	0.302	0
	$YbCoIn_5$ film	1.58	0.285	0
^{115}In(1)	$CeCoIn_5$ bulk	1.12	8.15	0
	$CeCoIn_5$ film	1.14	8.04	0
	$YbCoIn_5$ film	0.18	6.22	0
^{115}In(2)	$CeCoIn_5$ bulk	5.16	15.7	0.404
	$CeCoIn_5$ film	5.55	15.5	0.375
	$YbCoIn_5$ film	0.40	14.0	0.490

green arrows almost coincide with the peaks observed in the $CeCoIn_5$ and $YbCoIn_5$ thin films, respectively. The maximum at around 12.22 T observed in the $n = 5$ and 9 superlattices and the $YbCoIn_5$ thin film (asterisk and dashed peaks) is considered to be from the $CeIn_3$ buffer layer because such a peak around 12.22 T was not observed in the $CeCoIn_5$ thin film without the buffer layer. Owing to $\eta = 0$ and ν_{zz} parallel to the c axis at the In(1) site, central-transition peak ($+1/2 \leftrightarrow -1/2$) of the In(1) site is not shifted by the electric quadrupole interaction, but shifted by the hyperfine interaction related to the local spin susceptibility[25]. The Knight shift

$K(T)$ at the fixed frequency ω_0 is defined as

$$K(T) = \left(\frac{H_0 - H_{\rm res}}{H_{\rm res}}\right)_{\omega=\omega_0} = A_{\rm hf}\chi(T)$$

where $H_{\rm res}$ and H_0 are resonant magnetic fields of a sample and a bare nucleus that has the relation of $\omega_0 = \gamma_n H_0$ with the nuclear gyromagnetic ratio γ_n. $A_{\rm hf}$ and $\chi(T)$ are the hyperfine coupling constant and the local spin susceptibility, respectively. The shift from $\mu_0 H_0 = 12.27$ T ($K = 0$) is proportional to the Knight shift arising from the local static susceptibility at the In(1) site.

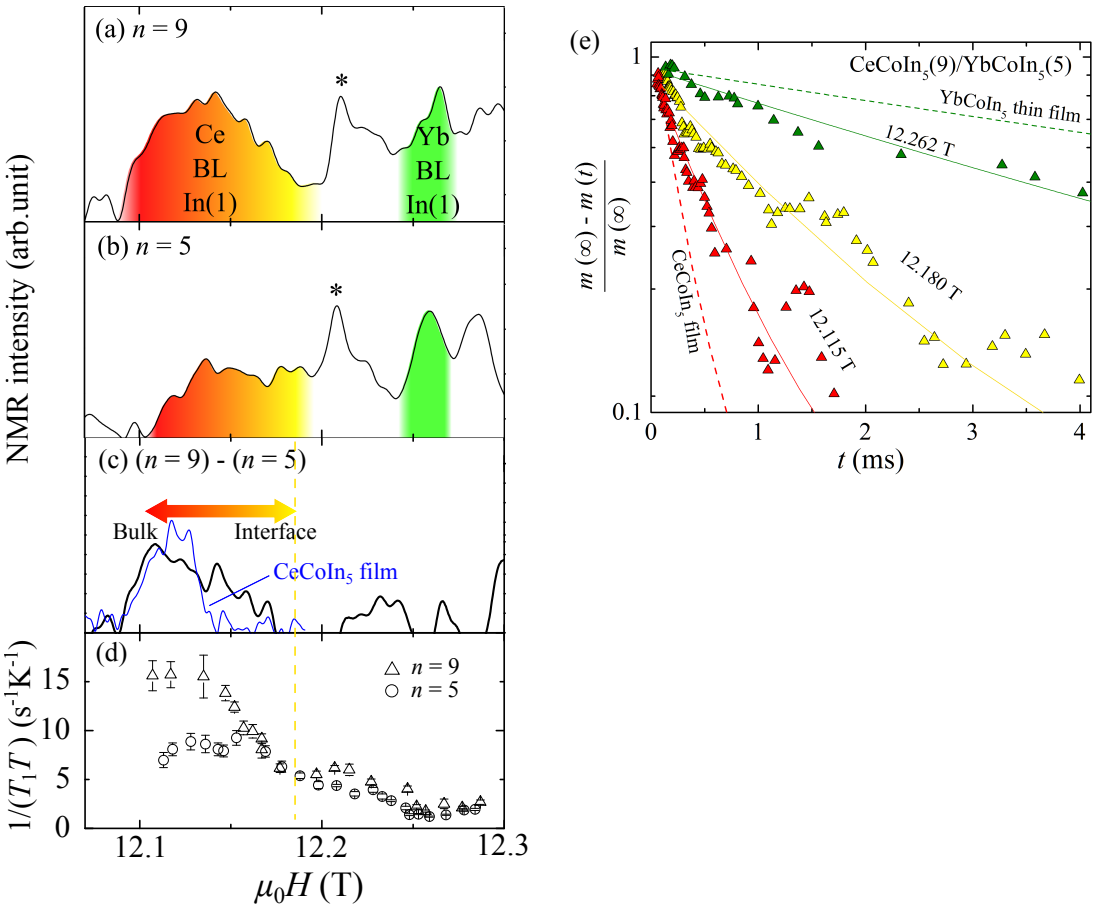

Figure 2. Field swept NMR spectra of the $n = 9$ (a) and $n = 5$ (b) superlattice samples at $T = 3.2$ K. (c) Subtraction of the spectrum of $n = 5$ sample from that of $n = 9$ sample. The NMR spectrum of $CeCoIn_5$ thin film is shown by blue line.(d) Field dependence of $(T_1T)^{-1}$ of the $n = 9$ and $n = 5$ samples. (e) Relaxation curves vs t plot at 12.262, 12.115, and 12.180 T in $CeCoIn_5(9)/YbCoIn_5(5)$ superlattice. The results of fitting are shown by solid line with each color as well as the $CeCoIn_5$ (red-dashed line) and $YbCoIn_5$ (green-dashed line) thin films.

Figures 2(a) and (b) depict the NMR spectra at 3.2 K at around the In(1) central transition of the $n = 9$ and $n = 5$ superlattices. The NMR spectra of these superlattices consist of signals from three different layers, i.e. Ce- and Yb-BLs and $CeIn_3$ buffer layers, each of which has different Knight shift. It should be stressed that the spectra arising from each layer are well separated in this field range. In FIGs. 2(a) and (b), the red to yellow gradient regions represent

the spectra of the Ce-BLs, the green regions represent the spectra of the Yb-BLs, and the peak pointed by asterisk is the spectra arising from $CeIn_3$ buffer layers. These assignments are made by the straightforward comparison with the spectra of $CeCoIn_5$ and $YbCoIn_5$ thin films. A salient feature is that the shape of the spectra of Ce-BLs for $n = 9$ is different from that of $n = 5$. The spectrum in the lower-field region for $n = 9$ has a much larger weight than that for $n = 5$. The lower-field signal indeed remains after the subtraction of the spectrum of $n = 5$ from that of $n = 9$, and it looks similar to the peak of the $CeCoIn_5$ thin film as shown in FIG. 2(c). The subtraction is considered to be the process which emphasizes the signal arising from the inner layers. Figure 3 indicates a schematic image of the subtraction. Here we labeled the layers of Ce-BL from "1" to "5" ("3") in $n = 9$ ($n = 5$). The layer "1" is the nearest layer to the Yb-BLs and the layer "2" is the next to the layer "1" as shown in FIG. 3. The number of the interfacial layers in Ce-BL should be the same in both of the $n = 9$ and $n = 5$ superlattices, and the difference between two superlattices is the number of the inner layers. The spectra arising from interfacial layers are canceled out by the subtraction of spectra of $n = 5$ from that of $n = 9$ and the remaining spectra in FIG. 2(c) is mainly arising from inner layer as shown in FIG. 3 (right). Thus, it is naturally concluded that the spectra in higher field regions shaded by yellow [FIG. 2(a) and (b)] arise from the outer $CeCoIn_5$ layers labeled "1" close to the interfaces and that the spectra in the lower field regions shaded by red arise from the inner $CeCoIn_5$ layers labeled "3" to "5".

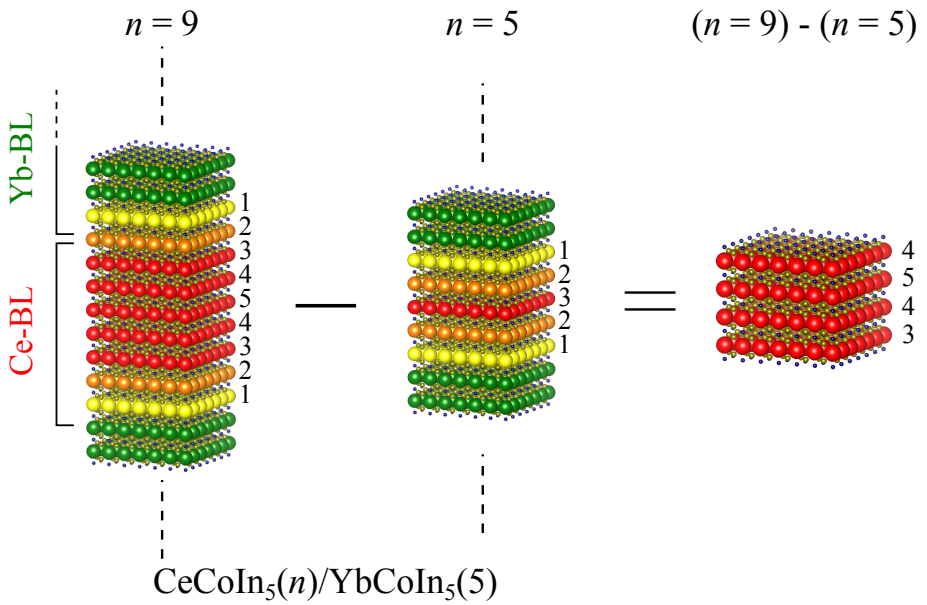

Figure 3. Schematic $CeCoIn_5$- and $YbCoIn_5$- layer arrangements in the superlattices $n = 9$(left) and $n = 5$(middle). The numbers shown at the right side of Ce-BLs represent the distance from the interfaces between Ce- and Yb-BL. In the subtraction $(n = 9)-(n = 5)$ (right), the numbered layers remain.

Next we discuss the field dependence of $(T_1T)^{-1}$ to resolve the layer dependence of the magnetic fluctuations even within a same Ce-BLs. Figure 2(d) depicts the field dependence of $1/T_1T$. The field dependence of $1/T_1T$ is clearly recognized from the recovery of the nuclear magnetization $m(t)$ at a time t after a saturation pulse(FIG.2 (e)). The recovery $(m(\infty) - m(t))/m(\infty)$ at 12.180 T (yellow triangles) is more slowly damped than the recovery at 12.115 T (red triangles). In the data of the $1/T_1T$s of FIG. 2(d), the $(m(\infty) - m(t))/m(\infty)$

curves were fitted by the function for central transition of nuclear spin $I = 9/2$ at the site with $\eta = 0$, given by

$$\begin{aligned}(m(\infty) - m(t))/m(\infty) = C\big[&0.0060606\exp(-t/T_1) + 0.033566\exp(-6t/T_1)\\ &+ 0.092308\exp(-15t/T_1) + 0.215\exp(-28t/T_1)\\ &+ 0.65306\exp(-45t/T_1)\big],\end{aligned}$$

where C and T_1 are fitting parameters[26]. The field dependence of $(T_1T)^{-1}$ indicates that AFM fluctuations which are dominant in bulk $CeCoIn_5$[22, 27] have strong spatial dependence even within the same Ce-BL ; fluctuations near at the interfacial layers are more suppressed than those at the inner $CeCoIn_5$ layers. At the inner layer signals around $\mu_0H = 12.115$ T, the $1/T_1T$ depends on Ce-BL thickness n i.e. the $1/T_1T$ increases with increasing n. On the other hand, at the interfacial signals around $\mu_0H = 12.180$ T, $1/T_1T$ is strongly suppressed and shows the same behavior in two superlattice samples. This is consistent with the fact that the number of interfacial layers are the same in both of $n = 9$ and $n = 5$ superlattices.

The observed suppression of the AFM fluctuations in the thinner Ce-BLs is opposite to the enhancement of fluctuations expected from two-dimensionalization. Taking into account of the spatial dependence of $1/T_1T$, it should be noted that the suppression of the AFM fluctuations is caused by effects of the interfaces. The suppression can be explained in terms of the effect of the breaking of local inversion symmetry at the interfaces between Ce- and Yb-BLs. In the presence of the local inversion symmetry breaking together with the fact that the Ce atom has a large atomic number, the Rashba-type spin-orbit coupling is expected to be strong in the present superlattices. The Fermi surface splitting due to the Rashba coupling should modify seriously the nesting condition and hence is expected to reduce the commensurate AFM fluctuations. With the reduction of n, the fraction of the noncentrosymmetric interface layers increases rapidly, leading to the suppression of the AFM fluctuations. The importance of the local inversion symmetry breaking at the interface has been emphasized experimentally through the peculiar angular variation of upper critical field, which can be interpreted as a strong suppression of the Pauli pair-breaking effect[19, 20]. The present results suggest that the local inversion symmetry breaking plays a key role for the magnetic properties at the interface, which is also consistent with the suppression of the superconductivity.

4. Conclusion

We have performed NMR measurements of $CeCoIn_5(n)/YbCoIn_5(5)$ superlattices with $n = 5$ and 9, as well as $CeCoIn_5$ and $YbCoIn_5$ thin films. By comparing the spectra of the superlattices with that of the thin films, we succeeded in identifying the ^{115}In NMR signals arising from the $CeCoIn_5$ and $YbCoIn_5$ layers in the superlattices, separately. Furthermore, we succeeded in distinguishing signals arising from interfacial and inner layers in Ce-BLs by comparing spectra of two superlattices which have different thickness of Ce-BLs. The suppression of $1/T_1T$ was prominent at the interfacial signals, which indicates that the AFM fluctuations at the interface are strongly suppressed than those of the bulk. The suppression of the AFM fluctuations is considered to be an intrinsic properties at the interface.

Acknowledgments

The authors thank S. K. Goh, R. Peters, Y. Tada, Y. Yanase and H. Ikeda for valuable discussions. This work was partially supported by Kyoto Univ. LTM center, Grant-in-Aid from the Ministry of Education, Culture, Sports, Science, Technology(MEXT) of Japan, Grants-in-Aid for Scientific Research (KAKENHI) from Japan Society for the Promotion of Science (JSPS), "J-Physics" (No. 15H05882, No. 15H05884, and No. 15K21732) and "Topological Quantum Phenomena" (No. 25103713) Grant-in-Aid for Scientific Research on Innovative Areas

from the MEXT of Japan, and by Grant-in-Aids for Scientific Research (Grants No. 25220710, and No. 15H05745). One of authors would like to acknowledge the support from the Motizuki Fund of Yukawa Memorial Foundation. Figures of crystal structures were shown using the VESTA package.[28]

References

[1] Fujimoto S 2005 *Phys. Rev. B* **72**(2) 024515
[2] Bauer E and MSigrist 2012 *Non-Centrosymmetric Superconductors: Introduction and Overview* (Springer, Heidelberg)
[3] Sato M, Takahashi Y and Fujimoto S 2009 *Phys. Rev. Lett.* **103**(2) 020401
[4] Sau J D, Lutchyn R M, Tewari S and Das Sarma S 2010 *Phys. Rev. Lett.* **104**(4) 040502
[5] Lutchyn R M, Sau J D and Das Sarma S 2010 *Phys. Rev. Lett.* **105**(7) 077001
[6] Hwang H Y, Iwasa Y, Kawasaki M, Keimer B and Nagao N 2012 *Nature materials* **11** 103–113
[7] Shishido H, Shibauchi T, Yasu K, Kato T, Kontani H, Terashima T and Matsuda Y 2010 *Science* **327** 980–983
[8] Mizukami Y, Shishido H, Shibauchi T, Shimozawa M, Yasumoto S, DWatanabe, Yamashita M, Ikeda H, Terashima T, Kontani H and Matsuda Y 2011 *Nature physics* **7** 849–853
[9] Ishii T, Toda R, Hanaoka Y, Tokiwa Y, Shimozawa M, Kasahara Y, Endo R, Terashima T, Nevidomskyy A H, Shibauchi T and Matsuda Y 2016 *Phys. Rev. Lett.* **116**(20) 206401
[10] Petrovic C, Pagliuso P G, Hundley M F, Movshovich R, Sarrao J L, Thompson J D, Fisk Z and Monthoux P 2001 *Journal of Physics: Condensed Matter* **13** L337
[11] Izawa K, Yamaguchi H, Matsuda Y, Shishido H, Settai R and Onuki Y 2001 *Phys. Rev. Lett.* **87**(5) 057002
[12] Stock C, Broholm C, Hudis J, Kang H J and Petrovic C 2008 *Phys. Rev. Lett.* **100**(8) 087001
[13] Zhou B B, Misra S, da Silva Neto E H, Aynajian P, Baumbach R E, Thompson J D, Bauer E D and Yazdani A 2013 *Nature physics* **9** 474–479
[14] Allan M P, Massee F, Morra D K, Dyke J V, Rost A, Mackenzie A P, Petrovic C and Davis J C 2013 *Nature physics* **9** 468–473
[15] Nicklas M, Stockert O, Park T, Habicht K, Kiefer K, Pham L D, Thompson J D, Fisk Z and Steglich F 2007 *Phys. Rev. B* **76**(5) 052401
[16] Booth C H, Bauer E D, Bianchi A D, Ronning F, Thompson J D, Sarrao J L, Cho J Y, Chan J Y, Capan C and Fisk Z 2009 *Phys. Rev. B* **79**(14) 144519
[17] Huy H T, Noguchi S, Hieu N V, Shao X, Sugimoto T and Ishida T 2009 *Journal of Magnetism and Magnetic Materials* **321** 2425 – 2428 ISSN 0304-8853
[18] Zaremba V I, Rodewald U C, Hoffmann R D, Kalychak Y M and Pottgen R 2003 *Zeitschrift fur anorganische und allgemeine Chemie* **629** 1157–1161 ISSN 1521-3749
[19] Goh S K, Mizukami Y, Shishido H, Watanabe D, Yasumoto S, Shimozawa M, Yamashita M, Terashima T, Yanase Y, Shibauchi T, Buzdin A I and Matsuda Y 2012 *Phys. Rev. Lett.* **109**(15) 157006
[20] Shimozawa M, Goh S K, Endo R, Kobayashi R, Watashige T, Mizukami Y, Ikeda H, Shishido H, Yanase Y, Terashima T, Shibauchi T and Matsuda Y 2014 *Phys. Rev. Lett.* **112**(15) 156404
[21] Yamanaka T, Shimozawa M, Endo R, Mizukami Y, Shishido H, Terashima T, Shibauchi T, Matsuda Y and Ishida K 2015 *Phys. Rev. B* **92**(24) 241105
[22] Kohori Y, Yamato Y, Iwamoto Y, Kohara T, Bauer E D, Maple M B and Sarrao J L 2001 *Phys. Rev. B* **64**(13) 134526
[23] Curro N J, Simovic B, Hammel P C, Pagliuso P G, Sarrao J L, Thompson J D and Martins G B 2001 *Phys. Rev. B* **64**(18) 180514
[24] Curro N J 2006 *New Journal of Physics* **8** 173
[25] Carter G C, Bennett L H and Kahan D J 1977 *Metallic Shifts in NMR* (Pergamon, Oxford)
[26] Narath A 1967 *Phys. Rev.* **162**(2) 320–332
[27] Sakai H, Brown S E, Baek S H, Ronning F, Bauer E D and Thompson J D 2011 *Phys. Rev. Lett.* **107**(13) 137001
[28] Momma K and Izumi F 2011 *Journal of Applied Crystallography* **44** 1272–1276 ISSN 1600-5767